第14卷 第2期 西北地震学报 Vol. 14, No. 2
1992年6月 NORTHWESTERN SEISMOLOGICAL JOURNAL June, 1992

THE RELATIONSHIPS BETWEEN EFFICACY OF GEOELECTRICAL RESISTIVITY METHOD IN EARTHQUAKE PREDICTION AND SITE CONDITION

Chen Youfa, Wang Defu*, Zhao Heyun,
Jiang Zhixiong*, Kang Yunsheng, Ding Hui

(Earthquake Research Institute of Lanzhou, SSB, China)

INTRODUCTION

In the past two decades, field observation, laboratory experiments, and the theoretical studies in the study on earthquake prediction have been carried out in several countries, by using ρ_s method, and valuable results have been achieved[1]—[11], [19]—[23].

The first geoelectrical resistivity (ρ_s) observatory for earthquake forecasting established at Litan, Hejian County of Hebei Province, China in 1967. Up to now, this method has undergone the following stages: initial experiment, great intermediate development, present—day generalization and perfection. Over 100 stations distributed along the North China and the South—North Seismic Belt have recorded in great detail the rich data concerning changes including geoelectrical resistivity and self potential, caused by both seismic and non— seismic activities. And this, in turn, has furnished evidence in many aspects for the estimation of the efficacy in predicting earthquake by ρ_s method.

Before discussing this problem it is necessary to concisely state the physical basis of ρ_s method which has been used in predicting earthquake. Based on the modern hypothesis on earthquake preparatory process, earthquake occurrence is due to the formation and development of the crustal rock mass crack—faults under the action of structural stress. In the evolution of crack the mechanical properties of the mass and environmental conditions of the mass may bring about obvious change, and gradually affect the physical (chemical as well) properties of the periphery mass, forming some abnormal regions. The mass resistivity is one of the sensors, most sensitive to the changes of mass stress state. Thus, the change of mass resistivity is inevitably caused in process of mass deformation and crack formation. Based on the Archie's Law

$$\rho_s = \rho_0 \varphi^{-m} S^{-n} \quad ,$$

(where ρ_0, φ, m, s and n are parameters of the rock), in the earthquake preparatory process the variations of those parameters may result in the change of ρ_s and become the precursors of earthquake[11]: Meanwhile, ρ_s method may gain the variation information of the mass resistivity in

* Seismological Bureau of Sichuan Province

depth, and exclude the near surface influence on the surveying result by surveying on the ground the apparent resistivity. So, the physical basis of ρ_s method in forecasting earthquake is clear. The following is mainly about the estimation of efficacy of ρ_s method in earthquake prediction.

THE ρ_s PRECURSORY CHARACTERISTICS ASSOCIATED WITH EARTHQUAKES

1. The ρ_s Precursory Characteristics Associated with Earthquakes 7 Magnitude

(1) The Phase Character in ρ_s Changes before and after Earthquakes

This is the most basic characteristic of ρ_s precursor. Fig. 1 shows the ρ_s phase character around the epicentre, taken from Changli and Baodi stations, before and after the 7.8 magnitude earthquake occurred in Tangshan on July 28, 1976. Fig. 2 shows the ρ_s variation curves around the epicentre, taken from Wudu station of Gansu province, before and after the two 7.2 magnitude earthquakes in Songpan—Pingwu on August 16 and 23 of 1976. Below N66.5°W (AB) is car bon slate which possesses high electric conductivity; N66.5° (CD) is close to the Bailong River. In 1983, PZ40 digital geoelectric meter replaced DDC—2 automatic electric compensator. The ρ_s pre cursors of the 7.9 magnitude earthquake in Luhuo

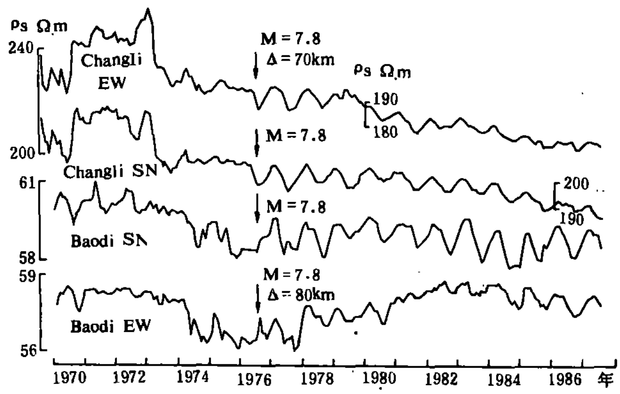

Fig. 1 Variation characteristics of pre— and post—seismic ρ_s phase property in Changli

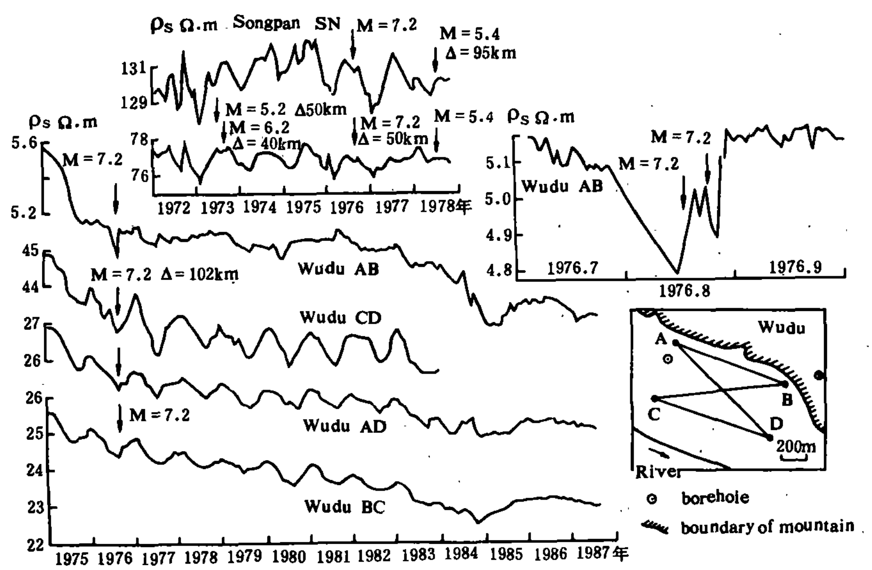

Fig. 2 Variation characteristics of pre— and post—seismic ρ_s phase property in Wudu and Songpan

on February 6, 1973 and of the 7.4 earthquake in Longling on May 29, 1976, are similar to the character mentioned magnitude above. From these cases it may be concluded that the chief tendency of dropping of ρ_s changes prior to the earthquakes above 7 in magnitude can be divided into six phases: 1) The normal change of ρ_s in earthquake —free phase; 2) Initial ρ_s dropping; 3) Recent gentle change of ρ_s; 4) High—speed dropping of ρ_s in a short time; 5) Abrupt change (earthquake occurrence) of ρ_s immediately prior to earthquakes; 6) Post—seismic regulating changes, as shown in Fig. 3. The characteristics of phase in ρ_s changes play a very important role in earthquake forecasting. If it could be accurately surveyed and judged, it will be possible to predict the existence of an earthquake or an evolving process of earthquake preparation in the regions under monitoring.

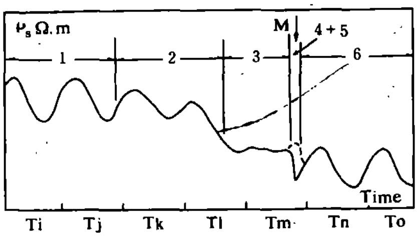

Fig. 3 The characteristics of phase in ρ_s changes

The characteristic of phase in ρ_s has gained support from other indications of the earthquake in Tangshan [12]. 1) From 1972 seismic frequency obviously began to rise. In 1973 the concentration was in Tangshan, Tianjin, and regions along the Bohai Sea coast and distributed along the north —east earthquake generation structure; 2) In 1972 b value began to increase and achieved its maximum in 1973, then decreased gradually, and rose again before the earthquake. 3) In the late period of 1973 the wave velocity ratio began to decline and only in the middle of 1974 did it gradually recover. By the end of 1975 it returned to the normal till the time when earthquake happened; 4) In 1972, the groundwater level began to drop gradually—became stable—and then quickened its decline, rose again after the earthquake; 5) The average Rn value began to rise in 1973 and returned to the normal after the earthquake; 6) The fault displacement quantity began to gradually rise in the middle of 1975— became stable—and returned to the normal after the earthquake; 7) The Z quantity component of geomagnetic field began to decline in the middle of 1975 with a range of over 10 gammas; 8) In the late period of 1975 the gravity value in Tangshan became larger compared with that in Beijing, with a range of 130 microgals

(2) The Regional ρ_s Decline before Earthquakes

Before the Tangshan 7.8 magnitude earthquake a negative value region of ρ_s precursors was formed around the epicentre of Tangshan earthquake with a length of about 300km from east to west and a width of about 140km from south to north, and the epicentre was where there was the maximal negative value of ρ_s precursors, as shown in Fig. 4. This characteristic is in accord with other indications of the Tangshan earthquake[12]: 1) There was general agreement between the structural stress field concentration area of the Tangshan earthquake judged from satellite gravity and the zero—value line of ρ_s indication contour map. The small stress region in Tangshan was located in the centre of the maximal value of ρ_s indications contour map. The direction of ρ_s indications were in agreement with those of the north—east to south—west seismic structural stress field in Tangshan; 2) The Tangshan rhombic scope was surrounded by the zero—value line of ρ_s indication contour map; 3) The aftershock distribution was in correspondence with the zero—value line position of ρ_s indication contour map; 4) The Z component of geomagnetic indications had Changli as their centre (it was closest to the epicentre); 5) The decline tendency of groundwater level was distributed in the direction of north to east.

(3) The Direction Character of ρ_s Indications before Earthquakes

From the gathered data of peripheral ρ_s indications of the Tangshan 7.8 magnitude earthquake it has been discovered that the change quantity $\Delta\rho_{sa}/\rho_s$ of different surveying directions at the same station varies. Despite the fact that the surveying directions of various local stations were not in complete agreement, and there were only two surveying directions, the dominant direction of such difference was obvious, as shown in Table 1. From the table we may see that the peripheral ρ_s indication change quantity of the Tangshan earthquake is that in area of N25°W—N42°E they are small (0.5—14%), while in the area of N69°E—S42°E they are large (2.6—17%). Using one-point-three-way iso-current separation equipment on the pillars 200m underground of a mine gallery in this country, it was observed that the ρ_s change quantity also had direction character under the condition of increase of mining pressure, as shown in Fig. 5. We see that the vertical (1) resistivity change quantity is minimal while the horizontal (2) change quantity is maximal, the slanting (3) is between the two. The angle between the local maximal pressure stress direction and the vertical direction is 10.2°; in other words, the minimal ρ_s variation direction is in general agreement with that of the principal compressive stress. Meanwhile, the amount of the ρ_s value has the same nature. It may reflect the stress state during the mass formation period.

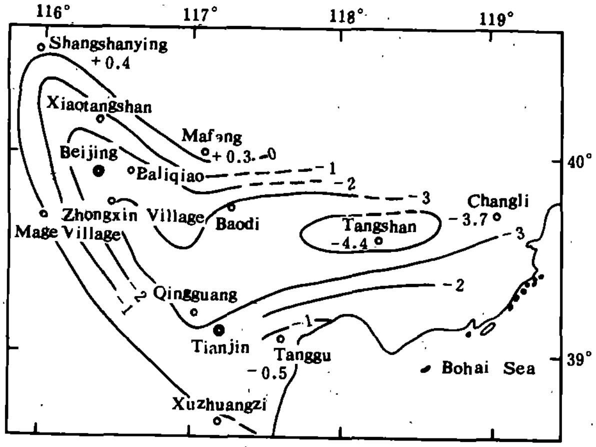

Fig. 4 Contour map of ρ_s precursor intensity $\Delta\rho_{sa}/\rho_s$ (south-to-north) in Beijing, Tianjin and Tangshan regions[5,12]

2. The Precursor of Intermediate Shocks

The gathered data show that the ρ_s indication characteristics of intermediate shocks ($5 \leqslant M \leqslant 6.9$) are less obvious than those of earthquakes over 7 magnitude. In general, their ρ_s precursor time is short, their range is small. The typical cases are shown in Fig. 2 and Fig. 6. Their ρ_s indicatons, however, are relatively obvious if the site condition of stations proves to be better and closer to the epicentre.

3. The statistical Relationships between ρ_s Indication characteristics and the Three Main Factors of Earthquakes

By means of the past two decades of experiment have cumulatively established the experimental and fixed quantity relationships between ρ_s indication characteristics and the three main factors of earthquakes.

(1) The Relationship between the ρ_s Precursor Time and Magnitude

From observations it is concluded that the longer the ρ_s precursor time T, the greater the magnitude M. Their relationship may be written as:

$$Log\ T = 0.34M + 0.13 \quad . \tag{1}$$

The unit of T is day . Their correlation coefficient is 0.99.

Table 1 Direction character of ρ_s mid and short arriving earthquake precursor of Tangshan 7.8 magnitude earthquake

Names of ρ_s station	Epicentral distance (km)	$\Delta\rho_{sa}/\rho_s$ (%)		Error of daily mean (%)	Distance of AB electrode, distance of MN electrode (m)
		SN	SN		
Tangshan	0	−4.5	−3.3	0.28	1000, 200
Changli	70	−0.5	−2.6	0.12	900, 217
Baodi	80	−3.0	−3.8	0.30	1000, 200
Zhongxin village	150	N42°E−3.9	N48°W−5.5	0.36	1000, 300
Majia valley	10	N25°W 5.0	N69°E 8.0	1.14	170, 20
Changli	70	2.4	3.0	0.12	900, 217
Xiji	120	14	17	0.68	2100, 380
Xuzhangzi	140	0	11	0.40	3000, 1000
Qing County	160	N30°E 0	N60°W 10	0.39	3200, 700

(2) The Relationship between the ρ_s Precursor Scope Δ and Magnitude

The gathered data show that the greater the earthquake, the broader the precursor scope. This may be expressed as:

$$Log\Delta = 0.29M + 0.50 \quad . \tag{2}$$

Where the unit of Δ is km, their correlation coefficient is 0.76.

(3) The Relationship between the ρ_s Precursor Time Scope and Magnitude

Due to the earthquake preparatory process continuously expanding toward the periphery from the source, the earthquake indications closely around the epicentre are observed earlier, with a prolonged tendency; while in farther regions the indications are observed later even only imminently before earthquake. Thus, when the magnitude M is fixed, at the stations near the epicentre, the precursor surveying time T will be longer, and T is shorter when Δ is big. Their relationship is

$$Log(\Delta \cdot T) = 0.59M + 0.69 \pm 0.36 \quad . \tag{3}$$

The correlation coefficient is 0.93.

(4) The Relationship between the ρ_s Precursor Quantity, Epicentral Distance, and Magnitude

Both theoretical analysis and actual results show that when the magnitude is fixed, the precursor quantity near the epicentral area is great; while that far from the area is small. The statistical relationship is

$$\Delta\rho_{sa}/\rho_s \cdot Log\Delta = 2.96M - 8.88 \quad . \tag{4}$$

Their correlation coefficient is 0.82.

(5) The Relationship between the ρ_s Precursor Quantity and Epicentral Distance

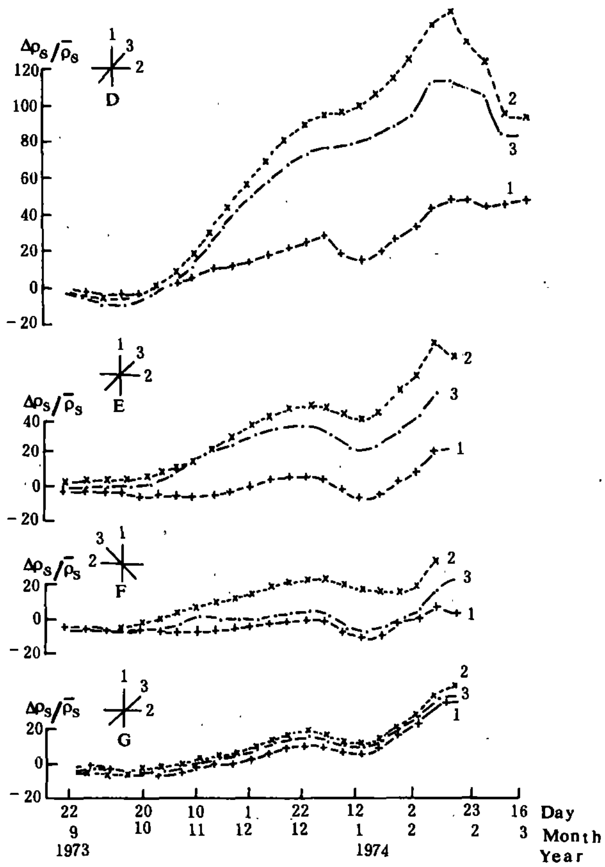

Fig. 5 Direction character of ρ_s variation on mine pillars

The ρ_s precursor quantity is abruptly reduced with the extension of epicentral distance. The statistical data of the Quaternary deposit (Q) with a thickness of less than 80m surrounding Tangshan, Luhuo, Yongshan—Daguan earthquakes show their relationship as:

$$\Delta\rho_{s\alpha}/\rho_s = 41.15\Delta - 1.5 \quad . \tag{5}$$

Their correlation coefficient is 0.91.

It should be pointed out that the acquisition of the ρ_s precursor time, space range and magnitude is not only related to the magnitude of earthquakes, but also related to ρ_s networks, the location of the ρ_s stations, and the precision of surveying instruments. The precision of the homemade DDC—2A automatic electric compensator is 1.5%. It may perceive strain of 10^{-6}. The corresponding ρ_s precursor quantity is 10^{-2}. From the data we get

$$\Delta = \frac{0.002L}{\sqrt[3]{\varepsilon_0}} + 54.4 \quad .$$

$$LogL = 0.47M - 1.57 \quad . \tag{6}$$

L is the fault length.

The unit of L is km. ε_0 is the minimal strain quantity of ρ_s precursor perceived by surveying instruments. PZ40 and ZD8 digital ρ_s instruments, with a precision of 0.02%, developed and manufactured in Lanzhou Seismological Institute, are gradually put to use at various local ρ_s stations. It is expected that this will improve the efficancy of ρ_s method in monitoring earthquakes[13].

To test the abovementioned statistical equations we use the data of the Tangshan

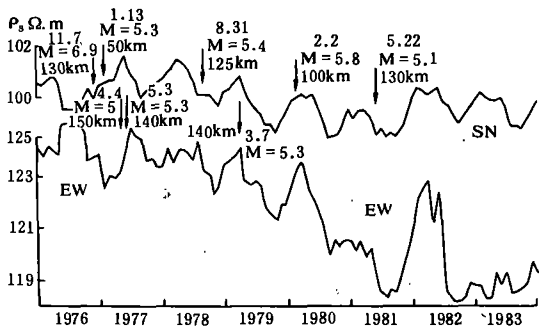

Fig. 6 Variation curves of ρ_s monthly mean at Xichang station

earthquake. The result is shown in Table 2. We see that the two are in general agreement.

Table 2 Related parameters (observed and calculated) of ρ_s precursor of the 7.8 magnitude Tangshan earthquake

Names of station	Epicentral distance (km)	$\Delta\rho_{sa}/\rho_s$ (%)		T (day)	
		Observed	Calculated	Observed	Calculated
Changli	70	5.6—5.9	7.7	1300	1358
Baodi	80	3.0—3.8	7.5	910	1188
Zhongxin village	150	3.9—5.5	6.5	600	634

THE FUNCTION OF THE ρ_s NORMAL CHANGE

In the acquired data, the ρ_s normal change has three states: 1) Normal annual change with the maximum value in March and the minimum value in September. More than 70% of the total number of ρ_s stations belong to this category; 2) Abnormal annual change with the minimum value in the former half of the year and the maximum value in the latter half. Less than 20% of the stations are in this category. The geoelectrical sections possessing $\rho_1 < \rho_2 > \rho_3$ within the body explored mll have abnormal annual change. These two kinds are the normal variations during earthquake — free period mentioned above. 3) The change of straight line type. From the data gathered at 98 ρ_s stations in this country we conclude that $\Delta\rho_{sy}/\bar{\rho}_{sy}$ change has directions. Its minimum value is in agreement with structural stress field direction[17—18]. Besides, the ρ_s normal change suggests that there is no seismic activity in the monitoring area. After the Luhuo earthquake in 1973, Tangshan, Longling, Songpan—Pingwu earthquakes in 1976, the ρ_s around them shows regular annual change state. In the recent ten years, no violent earthquakes occur in these areas, as shown in Fig. 1 and Fig. 2.

THE INFLUENCE OF THE ρ_s NETWORKS AND STATION LOCATION ON THE ρ_s INDICATION CHARACTERISTICS

In the estimation above an important factor has not been taken into consideration, that is, the influence of the ρ_s networks and station location on ρ_s indication characteristics. In fact, the position of the ρ_s networks, the density of stations and the structure of station sites, mechanics and hydrogeologic conditions of rock mass, surveying depths, the geoelectric sections, topography and landforms, electromagnetic interference and other conditions control the ρ_s indication characteristics and directly affect the efficacy of earthquake prediction by means of ρ_s method[14—16].

First, we believe it is necessary to set up networks in highly active seismic regions, especially those regions of subterranean medium with abnormal physical property and the regions close to active fault which have internal relationships with seismic pregnancy. The density of stations should be decided according to the magnitude of earthquakes under monitoring, the amount of the recorded $\Delta\rho_{sa}/\rho_s$ and the precursor time length. Equations (1)—(6) have provided evidence for the selection of the density of the ρ_s stations. Up to the moment, the influence of the location of the ρ_s stations on the ρ_s indication characteristics has not yet been clear. In the following sections we shall discuss several main problems concerning it.

1. The Influence of Earthquake Generation Structure

Observations show that those stations close to epicentre or to earthquake generation structure have longer time and bigger range of the ρ_s indications[15]. The Tangshan 7. 8 magnitude earthquake took place in the complicate structurally—locked area between the concealed fault and the poorly—connected Tangshan fault limited within the rhomb formed by Ninghe—Changli deep fault, Fengtai—Yejituo big fault, Luan County—Leting fault and Jiyun fault. Changli station is situated on Ninghe—Changli concealed deep fault. The ρ_s precursor time is longer and the range is bigger. The phase change is typically evident. While Baodi station is not located on the deep fault and far from the rhomb. The ρ_s indication characteristics are less obvious (The Quaternary deposit Q is thicker), as shown in Fig. 1. The 7. 2 magnitude Songpan—Pingwu earthquake occurred on the Huya fault eastside of Xuebaoding raised area. Songpan station is on the Minjiang fault westside of the area and flanked by two parallel faults which are not far from each other. Though it is 50km from the epicentre, the ρ_s indications are not obvious. Wudu station is 50km northeast from Huya fault and 102km away from the epicentre, the ρ_s precursor phase change characteristics have been obvious since the establishment in 1975, with a range of 2. 6—14%, as shown in Fig. 2.

2. The Influence of Mass Mechanics Property

ρ_s method is based on the survey of mass resistivity change caused by the change of mass stress—strain. Its object is the geologic body (mass) which has a certain structure and is in certain geologic and physical environments. The mass resistivity variation depends on the mechanical property and function of the mass proper; and the law of rock mechanics is influenced by its constituents, structure, and its environments (p, t, w). Different mass deformations and destructive mechanisms, the difference between mass resistance of deformation and destructive function, and the change of the environment the mass below a ρ_s station site all have a direct influence on the mass stress—strain—sensitivity of resistivity (or the resistivity change quantity per unit of stress strain $G_{\rho p} = \frac{\Delta\rho_{sa}/\rho_s}{P}$ $\frac{3X}{G_{\rho\varepsilon}} = \frac{\Delta\rho_{sa}/\rho_s}{\Delta L/L}$). The mechanical property of the Quaternary deposit Q is the poorest. It is table to be deformed by compressure, and turns quickly to partially densifying state. This is unfavorable to the transmission of stress and strain, and to the "absorbing" and "softening" of stress strain. In this way it controls seismic ρ_s precursor quantity. The thicker Q is, the more obvious the controling effect. Then Q is larger than 200m $\Delta\rho_{sa}/\rho_s$ is normally smaller than 2. 0%[14]. So this is one of the major interferences with ρ_s method. Table 3 shows the related statistical data of Tangshan and Songpan—Pingwu earthquake. It may be seen that at stations whose epicentral distances differ not much, $\Delta\rho_{sa}/\rho_s$ has obvious difference because normal change quantity $\Delta\rho_{sy}/\bar{\rho}_{sy}$ and resistivity state[14].

The influence of Q on $\Delta\rho_{sa}/\rho_s$ amount has been proved in the soil layer pressure experiments. The researchers at this Institute have done 24 such experiments on the natural soil layer in Lanzhou Observatory. The result of the loess layer experiments is that $G_{\rho\epsilon}=2.4-4.7\times10^2$; while in a certain mine 200—odd metres underground ρ_s method was with three directions of measure line to measure the changes of resistivity in silicide limestone under compression and it was found that $G_{\rho\epsilon}=8.4\times10^2$. The thinner Q is, the more regular the normal variation state becomes, and the greater amplitude, as shown in Table 4. Thus, the thick Quaternary system deposit should avoided when selecting ρ_s station sites.

Table 3a Related parameters around the 7.8 magnitudeTangshan earthquake

Names of station	Epicentral distance (km)	Thickness of regolith (m)	$\Delta\rho_{sa}/\rho_s$ (%)	AB, MN (m)	Geoelectric section
Tangshan	0	100	3.5—4.5	1000, 200	AK
Majia valley	10	10	12—24	170—260, 20	
Changli	70	70	5.6—5.9	900, 200—217	KH
Tanggu	80	>600	0.9—1.1	2000, 600	HK
Baodi	80	180	3.0—3.8	1000, 200	(H)K
Xiji	120	377	1.7—2.7	2100, 380	KH
Zhongxin village	150	80	3.9—5.5	1000, 380	HA

Table 3b Related parameters at Wudu station when the Songpan earthquake happened

Surveying direction	Regolith thickness (m)	Geoelectric sections	$\frac{AB}{2}$ when ρ_{smax} (m)	$\frac{AB}{2}$ when ρ_{smin} (m)	$\Delta\rho_{sa}/\rho_s$ (%)	AB, MN (m)
N66.5°W (AB)	20	HK	200	4	14.3	924, 308
N85°E (CB)		HK	210	31	4.2	1000, 333
N44°W (AD)		H		28	2.8	1000, 333
N66.5 W (CD)	100	HQ		20	2.6	924, 308

Table 4 The relationships between normal ρ_s variation and Q

Regolith thi-ckness (m)	Percentage of stations with normal annual variation (%)	Percentage of stations with abnormal annual variation (%)	Percentage of stations with irregular variation (%)	$\Delta\rho_{sy}/\bar{\rho}_{sy}$ (%)
≤200	50	4.2	45.8	<40
>200	25	25	50	<4.5

We used $G_\rho p$ as the comprehensive index to evaluate the influence of the mechanical property of diagenetic rock mass on ρ_s precursor. In a sense, the influence of the mechanical property of rock mass is the influence of rock mass porosity φ, temperature t, humidity w and pressure p on rock mass $G_\rho p$.

The great difference between rock mass and common substance lies in that the former is a poly—crack body with a certain texture and is cut vertically and horizontally by texture surface. The $G_{\rho p}$ of rock mass is naturally influenced by φ of such body as shown in Table 5[4]. From the table we see that $G_{\rho p}$ of the rock with $\varphi > 3\%$ is much smaller than that with $\varphi \leqslant 3\%$. The ρ_s precursor of such rock mass with large porosity, especially on the broken belt, is not obvious. From Archie's law we conclude that in the process of seismic pregnancy the ρ_s variation of part of the saturated rock mass has not only to do with φ and saturation s but also with porous fluid ρ_0, solidifying coefficient m and the index number n of s. So $G_{\rho P}$ variations are complex. Meanwhile Table 5 also shows that rock mass $G_{\rho P}$ diminishes as pressure increases.

Table 5 The relationships between $G_{\rho p}$ of rock mass and rock with its φ

$G_\rho P$, 10^{-3} \ P, b/cm² / Namse of rocks	100	250	500	Φ(10^{-3})
Maryland diabase	27.27	1.79	0.73	1
Rutland quartzite	4.49	3.89	1.89	5
Chittenden dolomite	4.66	2.68	1.84	10
Pottsville sandstone	4.80	4.09	2.72	29
Bedford limestone	0.21	0.28	0	120
Colorado tuff	0	0.23	0.28	400

The influence of moisture content filled in rock pore on ρ_s precursor is shown in Table 6[22]. From the table we know that $G_\rho P$ of rock mass does not have the maximum value when w is at its maximum or minimum, but at a certain w value. The experiments show that the density of water solution also has influence on $G_\rho P$ of rock mass as shown in Table 7. From the table we see that $G_\rho P$ (0.3) of rock mass saturated with 0.3Ω conductive water solution is larger than $G_\rho P$ (50) of that saturated with 50Ω water solution.

Table 6 The relationships between sandstone $G_\rho P$ and rock mass W under the single—direction pressure of 40—390kg/cm²

W(%)	$G_\rho P$ (10^{-3})	W(%)	$G_{\rho P}$ (10^{-3})
0.15	0.43	0.39	0.51
0.23	0.41	0.43	0.48
0.27	0.73	0.56	0.88
0.32	0.97	0.60	0.70
0.38	0.49	0.64	0.66

At the present moment the surveying depth of ρ_s method is several hundred metres or a little deeper: the temperature there has not much influence on rock mass grain ρ_s. In the range from 18 to 400°c, temperature variation does not change the essential relationships of rock mass ρ_s[22].

To sum up, the influence of the mechanical property and conditions of rock mass under ρ_s stations on ρ_s precursor is a complicated problem. It influences the basic characters of seismic presursor. In general, the exploring depth of ρ_s method is within 1km and within its exploring range it is complete rock mass ($\varphi<3\%$) in stead of broken geological bodies that can have better ρ_s precursor.

3. The Influence of Surveying Depth

From Table 3 we also see that with the increase of distance of AB electrode, the ρ_s precursor quantity gradually decreases. This reflects the influence of surveying depth on $\Delta\rho_{sa}/\rho_s$. The correlation field of the ρ_s normal change range and the current separation relationship are shown in Fig. 7. $\Delta\rho_{sy}/\bar{\rho}_{sy}$ greater than 30% is not indicated in the figure. We may also see that $\Delta\rho_{sy}/\bar{\rho}_{sy}$ decreases as AB increases. The survey result of resistivity on the pillars of a mine gallery has also proved this statement, shown in Table 8. Surveying depth influences the change quantity of $\Delta\rho_{sa}/\rho_s$ and $\Delta\rho_{sy}/\bar{\rho}_{sy}$. So, surveying depth of ρ_s method should not be too great as to influence surface electric change.

Table 7 The reljationships between water saturated rock mass $G_\rho P$ and water solution density

$G_{\rho}P\ 10^{-3}$ Items / P(b)	ρ_s(50)	ρ_s(0.3)	$\varphi(10^{-3})$
50—100	3.53	7.10	1.24
100—250	2.67	3.65	0.88
250—500	1.43	1.72	0.67
500—1000	0.95	1.01	0.32
1000—2000	0.86	0.79	0.04

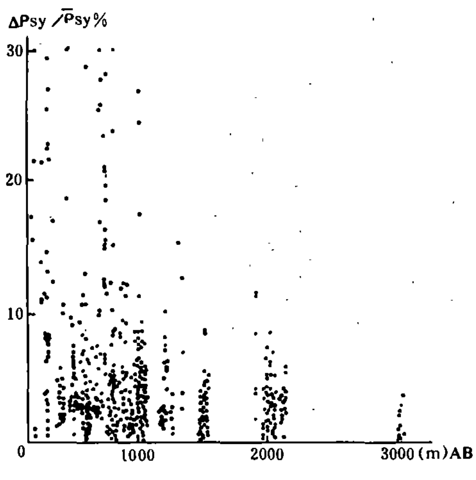

Fig. 7 Relationship between ρ_s normal change quatity and the distance of AB electrode

Strata of different ρ_s component influence not merely the surveying depth of ρ_s method and ρ_s variation states, but also cause greater surface interference so that to weaken the earthquake prediction efficacy of ρ_s method. The study of the relationships between geoelectric section types and ρ_s variation states at 36 ρ_s stations shows that ρ_s variatoin of K type ($\rho_1<\rho_2>\rho_3$) section of sites is in abnormal annual variation state; ρ_s of A type ($\rho_1<\rho_2<\rho_3$), AK type ($\rho_1<\rho_2<\rho_3>\rho_4$) and KHA type ($\rho_1<\rho_2>\rho_3>\rho_4<\rho_5$) of sites is basically in normal annual variatoin state; ρ_s of Q type ($\rho_1>\rho_2>\rho_3$), QH type ($\rho_1>\rho_2>\rho_3<\rho_4$) and HKH type ($\rho_1>\rho_2<\rho_3>\rho_4<\rho_5$) of sites is generally irregular; ρ_s of H type ($\rho_1>\rho_2<\rho_3$), HA type ($\rho_1>\rho_2<\rho_3<\rho_4$), HK type ($\rho_1>\rho_2<\rho_3>\rho_4$) and KH type ($\rho_1<\rho_2>\rho_3<\rho_4$) of sites has complex states. The relationships between geoelectric section types and seismic ρ_s precursor are shown in Table 9. From the table we conclude that the geoelectric sections reflecting earthquakes better are mostly those diagenetic rock strata with relatively higher resistivity in the bodies explored.

Table 8　Relationship between the $\Delta\rho_m/\rho_s$ mjeasured in the roof and the pillar in a mine funnel and the current separations

The roof			The pillar		
AB (m)	ρ_s (Ω. m)	$\Delta\rho_{sy}/\bar{\rho}_{sy}$ (%)	AB (m)	ρ_s (Ω. m)	$\Delta\rho_{sy}/\bar{\rho}_{sy}$ (%)
56. 6	90. 0	13. 7	12	300. 2	36. 6
35. 8	113. 6	16. 0	6	459. 3	48. 5
3. 25	1035. 3	48. 4	1. 5	643. 1	100. 2

Table 9　The relationships between geoelectric types and seismic $\Delta\rho_{ss}/\rho_s$

Names of stations	Geoelectric section	$L_{\rho_{smin}}$ (m)	$L_{\rho_{smax}}$ (m)	AB, MN (m)	Annual variation states	$\Delta\rho_{ss}/\rho_s$ (%)
Tangshan	HK	150	10	1000, 200	abnomal normal	3. 5—4. 5
Changli	KH	25	90	1000, 200	normal	2. 9—5. 6
Baodi	A			1000, 200	normal	3. 0—3. 8
Zhongxing village	HA		10	1000, 300	normal	3. 9—5. 5
Maja valley	A			260, 20	normal	5. 0—8. 0
Tanggu	HK	800	10	2000, 600	irregular	0. 9—1. 1

4. Hydrogeological Conditions

The medium under ρ_s stations can be divided into 3—phase (gas, liquid, solid) or 2—phase (liquid and solid or gas and solid) systems, namely, unsaturated, saturated, and dry rock masses. Experiments have proved that, by the action of pressure, ρ_s of these three types of rock mass shows different variation states, so ρ_s precursors are diversified. In this system, porous fluid plays a rather important role in ρ_s variation. It influences the amount of ρ_s value, and w, also influences $G_{\rho P}$ value of rock mass. Hydrogeological studies show that the opening cracks of rock mass below phreatic water surface are possibly filled with a certain amount of groundwater, and in the rock mass cracks above phreatic water surface (called osmotic belt) there is some moisture content to various degrees. During rainy and snowy seasons the moisture in the atmosphere falls onto the ground, reaches phreatic water surface by way of permeation to supplement groundwater and causes the rise of groundwater level; while in the season when it does not rain or snow, groundwater reaches the earth'surface by way of permeation and evaporates into the atmosphere. Thus the osmotic belt serves as the mutual supplementary channel between groundwater and atmospheric moisture. And the change in osmotic belt electric character comes to be one of the surface interference factors with ρ_s method. The permeability of rock mass is not as good as Q, so the surface interference effect of Q is stronger than that of rock mass. This requires a deeper deposit of groundwater under station sites. The relationships between groundwater level variation and ρ_s are quite complex. At Jiayuguan station in Gansu Province, ρ_s shows abnormal annual variation state, it shares a mirror image relationship with the groundwater level variation in the same place; while in Pixian County of Sichuan Province ρ_s also shows the same state, but goes synchronously with groundwater level variation there. One common characteristic they share is that the geoelectric sections are the same (of K type).

CONCLUSION

To sum up, ρ_s method has promising prospect in monitoring seismic activities above 7 magnitude under the present technical conditions. It has recorded indication characteristics having such properties of long time, wide range, obvious phases. It can also succeed in surveying the ρ_s indications of intermediate earthquakes if the ρ_s networks are located properly, the density of stations is moderate, and the location of stations is in good condition. Most of our ρ_s stations were set up in the first half of the 1970s, the selection of networks and station sites was lack of theoretical guide then, so the conditions of ρ_s station sites, especially the thickness of the Quaternary deposit differs greatly. And this results in the complicated ρ_s change states. To estimate ρ_s method under such conditions in forecasting earthquakes would be likely to go astray. In the future research work, we should emphasize the study of seismic ρ_s indications; and what is more, we should pay close attention to the study of the relationships between seismic ρ_s indication characteristics (including the ρ_s normal change), the ρ_s networks, as well as the condition of station sites.

Reference

〔1〕Y. Yamazaki, Bull. Earthq. Res. Inst., 55, 1980.
〔2〕Y. Yamazaki, Bull. Earthq. Res. Inst., 58, 1983.
〔3〕A. Mazzella et al., Science, 185, 1974.
〔4〕W. F. Brace et al., J. Geophys. Res., Vol. 73, No. 16, 1968.
〔5〕Qian Jiadong et al., Earthquake Prediction, pp. 145—155, 1982.
〔6〕Qian Jiadong, Chen Youfa et al., Applications of Geoelectrical Resistivity in Earthquake Prediction (chinese), Seismological Press, China, 1985.
〔7〕Qian Fuye et al., Scientia Sinica, No. B9, 1982.
〔8〕Zhang Tongjun, Northwestern Seismological Journal, Vol. 3, No. 1, 1981.
〔9〕T. Yukatake et al., Bull. Earthq. Res. Inst., 53, 1978.
〔10〕Chen Youfa, Northwestern Seismological Journal, Vol. 8, No. 4, 1986.
〔11〕Chen Youfa, Northeastern Seismological Research, Vol. 3, No. 3, 1987.
〔12〕The Editoral Group of "1976 Tangshan Earthquake", SSB, 1976 Tangshan Earthquake (Chinese), Seismological Press, China, 1982.
〔13〕Zhao Jialiu et al., Northwestern Seismological Journal, Vol. 4, No. 2, 1982.
〔14〕Chen Youfa et al., Northwestern Seismological Journal, Vol. 4, No. 2, 1982.
〔15〕Chen Youfa et al., Northwestern Seismological Journal, Vol. 6, No. 3, 1984.
〔16〕Chen Youfa et al., Northwestern Seismological Journal, Vol. 8, No. 2, 1986.
〔17〕Chen Youfa et al., Northwestern Seismological Journal, Vol. 1, No. 3, 1979.
〔18〕Chen Youfa et al., Acta Seismologica Sinica, Vol. 3, No. 1, 1981.
〔19〕О. М.Барсуков, Земля и Вселенная, No. 6, 1979.
〔20〕А. Я. Сидорин, доклады, 290, No1, 1986.
〔21〕А. А. Анапимов и др., Доклады, 263, No. 2, 1982.
〔22〕Э. И. Пархоменко, Электрические свойства горных пород, 1965.
〔23〕Н. Л. Нерсесов и др., Физика Земли, 4, 1982.